ETB 3 – THERMOSOLAR DESIGN

Joseph Jolley

Jrj44

WORD COUNT: 2407 (excluding references, list of figures & tables)

Abstract

This project produces a solar irradiance estimate for a flat plate collector system located in Marrakech, Morocco. During June, the average irradiance during daylight hours can reach $\sim 600W/m^2$, in comparison to December where the average is $\sim 315W/m^2$. Using this information a Lithium Bromide cooling absorption cycle (LiBr-H_2O) was designed to maintain the internal temperature of a 3-bedroom house at $20°C$ with the external temperature reaching up to $36°C$ (hence cooling a 3-bedroom house). This system requires $15.88m^2$ of flat plate solar thermal collectors for sufficient cooling, during the intense external atmospheric temperature periods. Furthermore, genetic algorithms were employed to optimise coefficient of performance (COP) of the LiBr-H_2O cycle, with the; upper pressure, lower pressure, upper and lower concentrations of the LiBr, all being variables. The final cooling design achieved a COP of 0.85.

Contents

List of Figures

List of Tables

1. Introduction

This document has 2 key sections. The first section is on the calculation of solar irradiance at the Marrakech, Morocco location. The second section is on the flat plate collector design for the cooling of a 3-bedroom house, along with the absorption cooling cycle design.

Additionally, a .py code file has been attached upon submission, please download, and run the code. For the modelling of the Solar vapor compression (VC) cycle and Lithium bromide absorption cycle (the conjunction between the VC and absorption cycle will be explained in Section 3.2), several equations from the International Association for the Properties of Water and Steam (IAPWS) (2012) and Faruque, MD (ASHRAE, 2021) were referenced and used. For any control volume in either cycle (VC or absorption), the mass flow and energy balance have been satisfied.

2. Daily, monthly and yearly solar Irradiance estimate – Morrocco Marrakech

2.1 Calculation Steps

The location of Morrocco Marrakech is (latlong.info):

- $Latitude = 31.63° \ (\emptyset)$
- $Longitude = \ -8.078°$
- $Sea\ Level\ Elevation = 0.468\ km\ (A)$

Firstly, defining the Equation of Time (EoT), this accounts for the difference between the true solar time, and the mean solar time for a specified date, N, which is referred to as the 'day number' within a year, ranging from 1 – 365 (PowerFromTheSun, Chapter 3.1).

$$EoT = 229.2(0.000075 + 0.001868\cos(B) - 0.032077\sin(B) - 0.014615\cos(2B) - 0.04089\sin(2B)) \quad (Eq\ 1)$$

Where $B = \frac{360(N-1)}{365} \quad (Eq\ 2)$.

Secondly, the solar time is defined as (PowerFromTheSun, equation 3.5):

$$t_s = \frac{4(LSTM - Longitude) + EoT}{60} + standard\ time \quad (Eq\ 3)$$

Where,

- $LSTM = UTC \times 15$ is a time correction factor.
- $Standard\ time$ is registered in hours, and can be selected by the user, this must be within the range of 0 – 24, representing the 24-hour clock. This is particularly useful when calculating the average irradiance for the day via integrating over the 24 hours, then dividing by the number of time steps used to sum for the total irradiance.

t_s above is in hours, and needs to be converted into degrees:

$$\omega = 15(t_s - 12) \quad (Eq\ 4)$$

Before calculating the zenith (θ_z), the declination angle (δ) must be defined (PowerFromTheSun, equation 3.7):

$$\delta = 23.45\sin\left(\frac{360}{365}(284 + N)\right) \quad (Eq\ 5)$$

Therefore, the zenith angle is (PowerFromTheSun, equation 3.17):

$$\theta_z = cos^{-1}(\cos(\delta)\cos(\omega)\cos(\emptyset) + \sin(\delta)\sin(\emptyset) \quad (Eq\ 6)$$

Using Hottel's Model, the diffuse solar irradiance $(I_{d,h})$ and direct normal solar irradiance $(I_{b,n})$ is calculated respectively, via (PowerFromTheSun, equation 2.15):

$$I_{d,h} = I_O \cos(\theta_z)(0.2710 - 0.2939\left(a_0 + a_1 e^{(-ksec(\theta_z))}\right) \quad (Eq\ 7)$$

$$I_{b,n} = I_O\left(a_0 + a_1 e^{-ksec(\theta_z)}\right) \quad Eq\ (8)$$

Where from Hottel's Model:

$$a_0 = 0.4237 - 0.00821(6 - A)^2$$

$$a_1 = 0.5055 + 0.00595(6.5 - A)^2$$

$$k = 0.2711 + 0.01858(2.5 - A)^2$$

$$A = Elevation\ from\ sea\ level\ (km)$$

Therefore, by applying the cosine effect to the direct normal solar irradiance, the total irradiance can be calculated for any $Standard\ time$ and any day number (N) via:

$$I_{t,h} = I_{b,n}\cos(\theta_z) + I_{d,h} \quad (Eq\ 9)$$

2.2. Irradiance results

To estimate the daily results, the equations 1, 2, and 5 need to be calculated once for each day, then the hourly $standard\ time \in [0,24]$ simply needs to be iterated over, and the equations 3, 4, 6, 7, 8, 9 all need to be re-calculated for each iteration, with the result appended to a list. Additionally, if $|\theta_z| > 90°$, this signifies the sun is not in direct sight of the collector, and the equations return 0, in contrast to a $-ve$ value if this was not accounted for.

2.2.1 Intraday Irradiance

Figures 1 and 2 show the intraday irradiance for June 21st and December 21st respectively.

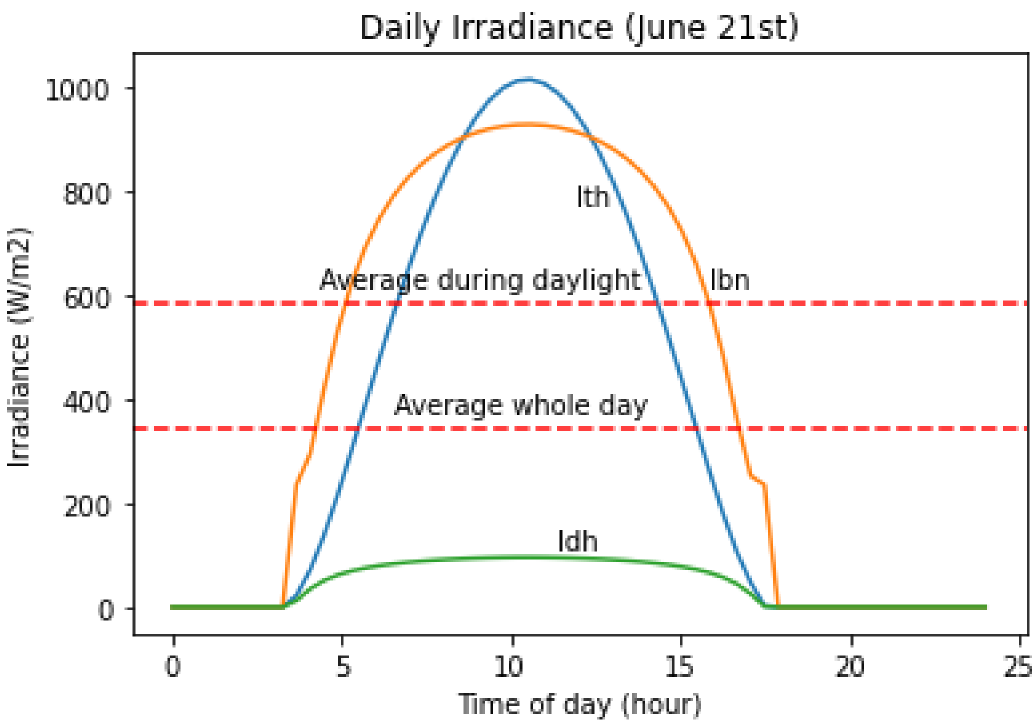

Figure 1: Morocco Marrakech Intraday Irradiance - June 21st.

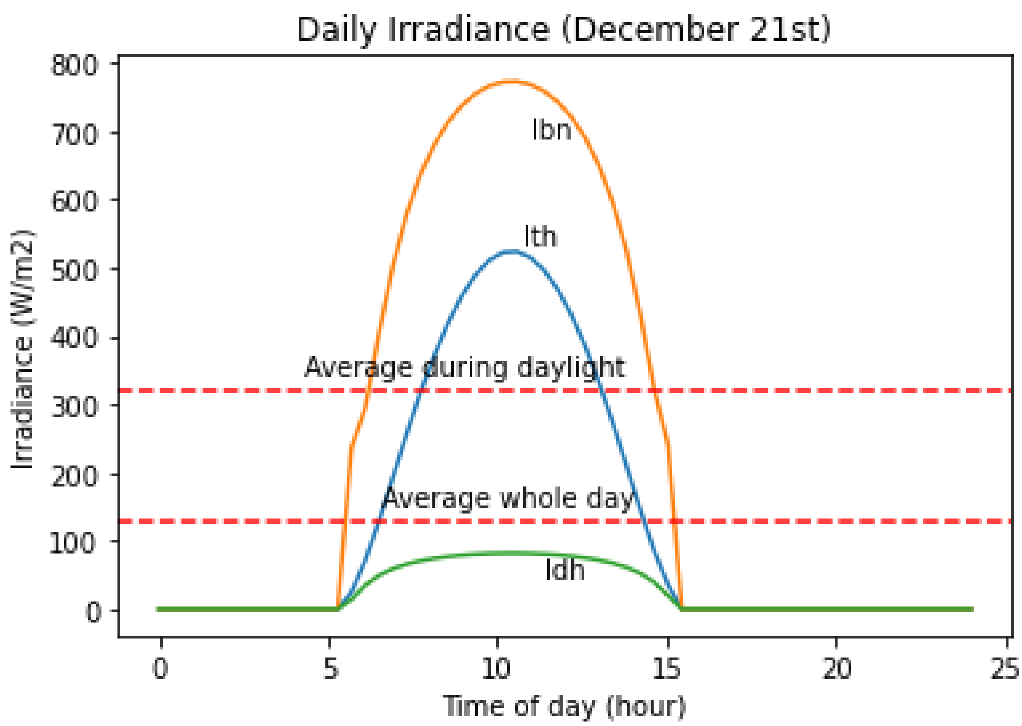

Figure 2: Morocco Marrakech Intraday Irradiance - December 21st

2.2.2 Daily and Monthly Irradiance Throughout a Year

Figure 3 shows the average daily irradiance during daylight hours throughout a year, whilst Figure 4 shows the monthly average daily irradiance during daylight hours. Figure 3 has an unsmooth line, this is simply due to the period of daylight hours not being equal throughout the year, increasing the number of datapoints during the 'for' loop over the $standard\ time \in [0,24]$ will have resulted in a smoother line, but with greater time complexity.

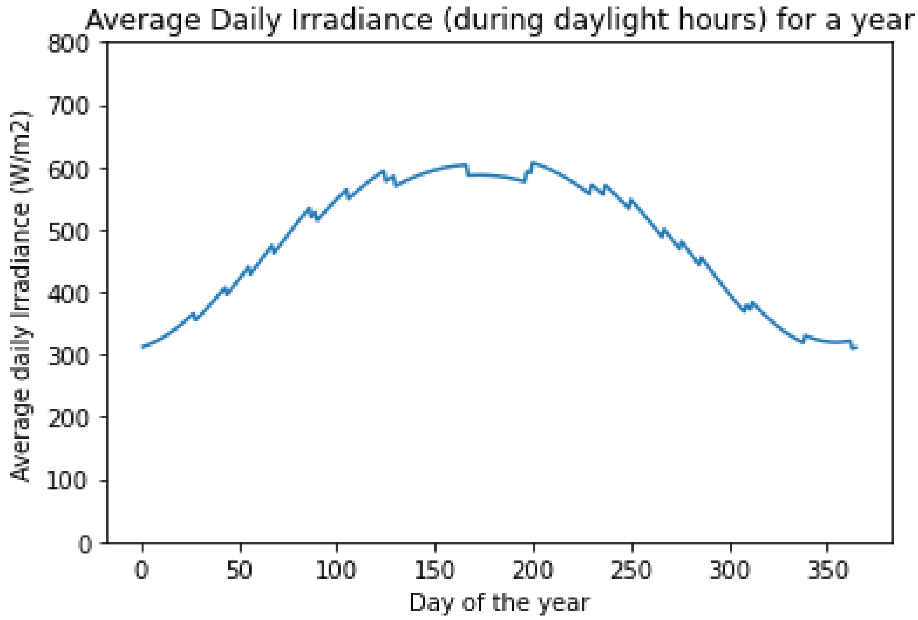

Figure 3: Average daily irradiance during daylight hours throughout a year.

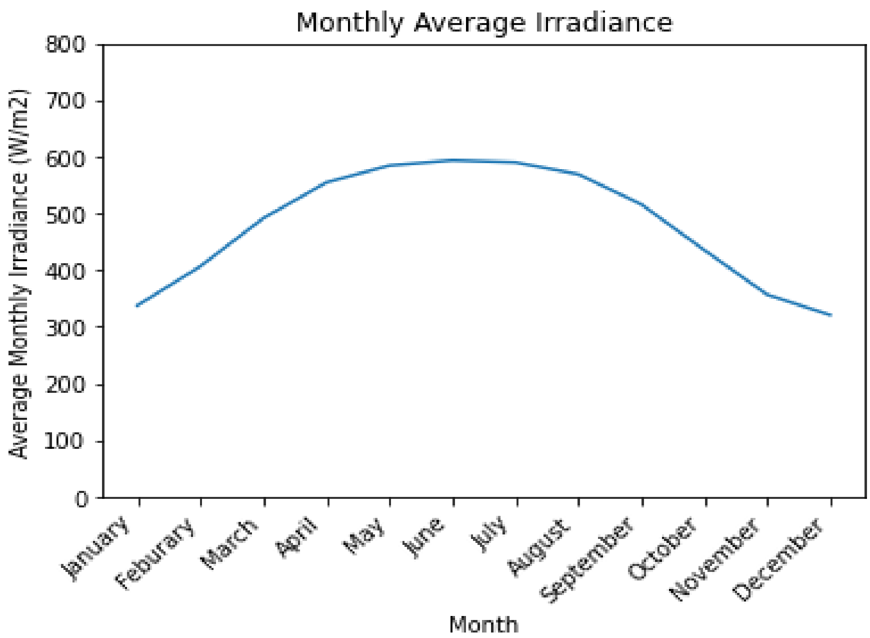

Figure 4: Average monthly irradiance throughout a year.

3. Flat Plate Collector – 3 Bedroom Cooling

3.1 House Cooling Load Calculation

Firstly, to design and size the flat plates collectors, the cooling load for the 3-bedroom property must be calculated first. The calculations are summarised in Table 1, the design is to operate on a hot day in July and will use the daily average irradiance during sunlight hours (for July) to calculate the size of plate collectors required, as the cooling effect during nighttime is not required and that the majority of the irradiance comes from (direct irradiance) during daylight hours.

- $Outdoor\ Temperature =\ 36°C$ (Weather Atlas)
- $Desired\ indoor\ temperature = 20°C$

From the wet and dry bulb temperatures in Morocco from July and using the psychrometric chart, the humidity ratio is ~0.015 kg/kg (Evapopedia. 2014). Using this information and assuming the property has relatively good airtightness, the latent load factor is: 1.16 (COECS.edu).

Table 1: 3-bedroom cooling load (kW) estimate - Morocco

	Quantity	Load Factors $\left(\frac{W}{person}\right)$ or $\left(\frac{W}{m^2K}\right)$	Cooling Load (kW)	References
People	4 people resting	60	0.24	ASHRAE 55. 2010.
Door Area (Oak Hardwood)	4.22m^2	6.78	0.46	ASHRAE U-values. 2021.
Wall Area (cavity brick)	170m^2	0.87	2.37	MCS U-values. 2019.
Floor/Roof Area	70m^2	0.37	0.41	MCS U-values. 2019.
Window Area (single glazed)	20m^2	4.8	1.54	MCS U-values. 2019.
Total (kW)			5.01	
Latent Load Factor			1.16	
Safety Factor			1.3	
Cooling Load Required (kW)			7.56	

Therefore, the house cooling load required for a hot day in July is 7.56kW, including a safety factor in case of any poor assumptions.

3.2 LiBr-H_2O absorption cooling cycle design.

The design of the LiBr-H_2O cooling cycle (view Figure 5) must take in 7.56kW across its evaporator within the house environment (to ensure sufficient cooling effect which was calculated in section 3.1). Using this information, along with upper and lower pressures and LiBr (%) concentrations of the system, and a mass flow rate, the energy provided to the generator (Q_g) within the LiBr-H_2O cycle can be calculated. The energy provided to the generator comes from a high temperature superheated vapor from a separate vapor compression-expansion cycle, this vapor compression-expansion cycle absorbs solar thermal energy across its evaporator. The primary reason for the use of a vapor compression cycle in place of the solar thermal energy being directly captured by the generator is that; the solar thermal energy alone will not be sufficiently concentrated to manipulate the necessary phase changes of the LiBr-H_2O working fluid, whereby using a vapor compression cycle, phase manipulation and superheated steam can be produced in the LiBr-H_2O cycle. Simply put, the vapor compression cycle allows the system to concentrate the solar energy into a superheated vapor (stream 2), which can then be used to provide energy to the generator of the LiBr-H_2O cycle.

This design was inspired by Assad MEH, et al (2021), but with the change of location from UAE to Morocco, and changing the source energy from geothermal, to solar thermal, and finally changing some operational parameters (upper and lower pressures of the system, mass flow, and concentrations of LiBr). Furthermore, the working fluid includes LiBr-H_2O with H_2O refrigerant, which are non-toxic, and has a relatively high latent heat, and in Morocco the cooling cycle has no concern of temperatures dropping below 0℃ (Assad MEH, et al. 2021).

Figure 5 shows the schematic layout for the solar thermal absorption cooling cycle, which is made up from a vapor compression cycle (streams 1,2,3, and 4) and a LiBr-H_2O absorption cooling cycle (streams 5, 6, 7, 8, 9, 10, 11, 12, 13, and 14).

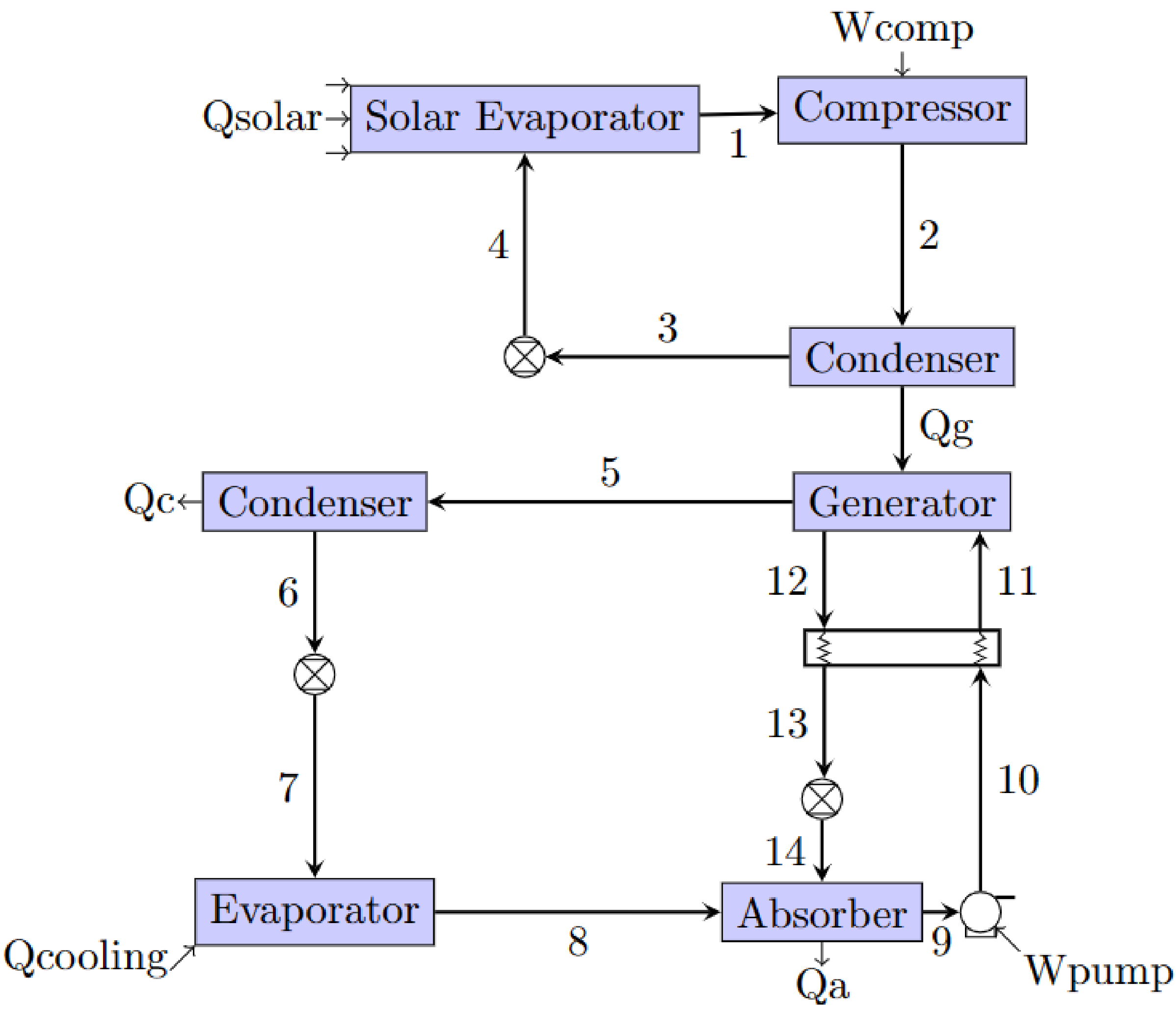

Figure 5: Solar Thermal - Vapor compression cycle - LiBr-H2O cooling cycle.

Table 2 shows the fundamental equations used to calculate the different stream parameters. The cells shaded in light green, and light blue show the equations for the vapor compression cycle and LiBr-H_2O cycle, respectively.

Table 2: System of Equations

Equipment	**Mass Balance**	**Energy Balance**
Solar Evaporator	$\dot{m}_4 = \dot{m}_1$	$Q_{solar} + \dot{m}_4 h_4 = \dot{m}_1 h_1$
Compressor	$\dot{m}_1 = \dot{m}_2$	$W_{comp} + \dot{m}_1 h_1 = \dot{m}_2 h_2$
Condenser	$\dot{m}_2 = \dot{m}_3$	$\dot{m}_2 h_2 = Q_g + \dot{m}_3 h_3$
Expansion Value	$\dot{m}_3 = \dot{m}_4$	$\dot{m}_3 h_3 = \dot{m}_4 h_4$
Condenser	$\dot{m}_5 = \dot{m}_6$	$\dot{m}_5 h_5 = Q_c + \dot{m}_6 h_6$
Expansion valve 1	$\dot{m}_6 = \dot{m}_7$	$\dot{m}_6 h_6 = \dot{m}_7 h_7$
Evaporator	$\dot{m}_7 = \dot{m}_8$	$Q_{cooling} + \dot{m}_7 h_7 = \dot{m}_8 h_8$
Absorber	$\dot{m}_8 + \dot{m}_{14} = \dot{m}_9$	$\dot{m}_8 h_8 + \dot{m}_{14} h_{14} = Q_a + \dot{m}_9 h_9$
Pump	$\dot{m}_9 = \dot{m}_{10}$	$\dot{m}_9 h_9 + W_{pump} = \dot{m}_{10} h_{10}$

Embedded heat exchanger	$\dot{m}_{10} = \dot{m}_{11}$ $\dot{m}_{12} = \dot{m}_{13}$	$\dot{m}_{10}h_{10} = \dot{m}_{11}h_{11}$ $\dot{m}_{12}h_{12} = \dot{m}_{13}h_{13}$
Generator	$\dot{m}_{11} = \dot{m}_{12} + \dot{m}_5$	$Q_g + \dot{m}_{11}h_{11} = \dot{m}_{12}h_{12} + \dot{m}_5h_5$
Expansion valve 2	$\dot{m}_{13} = \dot{m}_{14}$	$\dot{m}_{13}h_{13} = \dot{m}_{14}h_{14}$

The LiBr-H_2O cycle was designed first, by working backwards from the cooling load, to calculate the energy input required by the generator (labelled Q_g in Figure 5), which can then be used to size the flat plat collects and design the vapor compression values.

For the LiBr-H_2O system to operate there are infinite solutions to the system of equations, hence allowing flexibility when selecting operating parameters for the system. The parameters for the LiBr-H_2O system which can be selected, include; lower system pressure, upper system pressure, lower LiBr concentration and upper LiBr concentration. The performance of an LiBr-H_2O absorption cooling system is determined by the coefficient of performance, 'COP', calculated via (Assad MEH, et al. 2021) (noticeably, the W_{pump} has not been included, therefore not highlighting the total performance, likely due to different energy grades):

$$COP_{LiBr-H_2O} = \frac{Q_{evaporator}}{Q_{generator}}$$

In contrast to testing all the system parameters with various combinations (through coordinate ascent), which would lead to time complexity $O(n^4)$, a genetic algorithm (GA) was employed to optimise for the COP objective function above, several 'subject to' constraints were also employed, limiting the pressure ranges and concentration (to suit vacuum conditions, and recommended ranges from the ASHRAE equations):

$$\max COP_{LiBr-H_2O}$$

Furthermore, once the $Q_{generator}$ has been calculated the vapor compression cycle operating conditions can be calculated in a similar manner. The parameters of the vapor compression system to select, include; upper pressure, lower pressure, and mass flow rate, this would lead to a time complexity of $O(n^3)$ to run a coordinate ascent/descent algorithm. A second GA was employed, with the objective function to maximise being (this will increase the solar energy capture required, but minimises the electrical work from the compressor required):

$$\max \frac{1}{W_{comp}}$$

Several 'subject to' constraints were employed on the upper pressure, lower pressure, and mass flow for the system.

The final values for mass flows, enthalpies, pressures, concentrations of LiBr, and stream phase has been highlighted in Table 3 (calculated via the .py code attached), the vapor compression parameters and LiBr-H_2O parameters are highlighted in light green and light blue, respectively. In addition, PH diagrams have been plotted for the vapor compression streams and LiBr-H_2O streams, in Figures 6 and 7 respectively. Both the cycles have a lower and upper pressure which is considered a vacuum (<100kPa), improving practical feasibility.

Table 3: System parameters

Stream	Mass flow ($\frac{kg}{s}$)	Pressure (kPa)	Temperature (℃)	Enthalpy ($\frac{kJ}{kg}$)	LiBr concentration (%)	Phase
1	0.0037	19.76	59.80	2608.49	-	Saturated vapor, low P.
2	0.0037	20.77	106.43	2650.40	-	Superheated vapor, high P.
3	0.0037	20.77	60.88	254.83	-	Saturated liquid, high P.
4	0.0037	19.76	59.80	254.83	-	Vapor-liquid mixture, low P.
5	0.0032	6.00	38.16	2570.50	-	Superheated water vapor, high pressure.
6	0.0032	6.00	36.16	151.49	-	Saturated liquid water, high pressure.
7	0.0032	0.68	1.48	151.49	-	Saturated water-vapor mixture, low pressure.
8	0.0032	0.68	1.48	2503.61	-	Saturated water vapor, low pressure.
9	0.0161	0.68	9.77	9.00	40.0	Saturated solution, low P.
10	0.0161	6.00	9.77	10.25	40.0	Sub-cooled liquid solution, high P.
11	0.0161	6.00	86.43	62.93	40.0	Sub-cooled liquid solution, high P.
12	0.0129	6.00	59.80	125.46	50.0	Saturated liquid solution, high P.

13	0.0129	6.00	33.64	59.61	50.0	Sub-cooled liquid solution, high P.
14	0.0129	0.68	21.23	59.61	50.0	Vapor-liquid solution, low P.

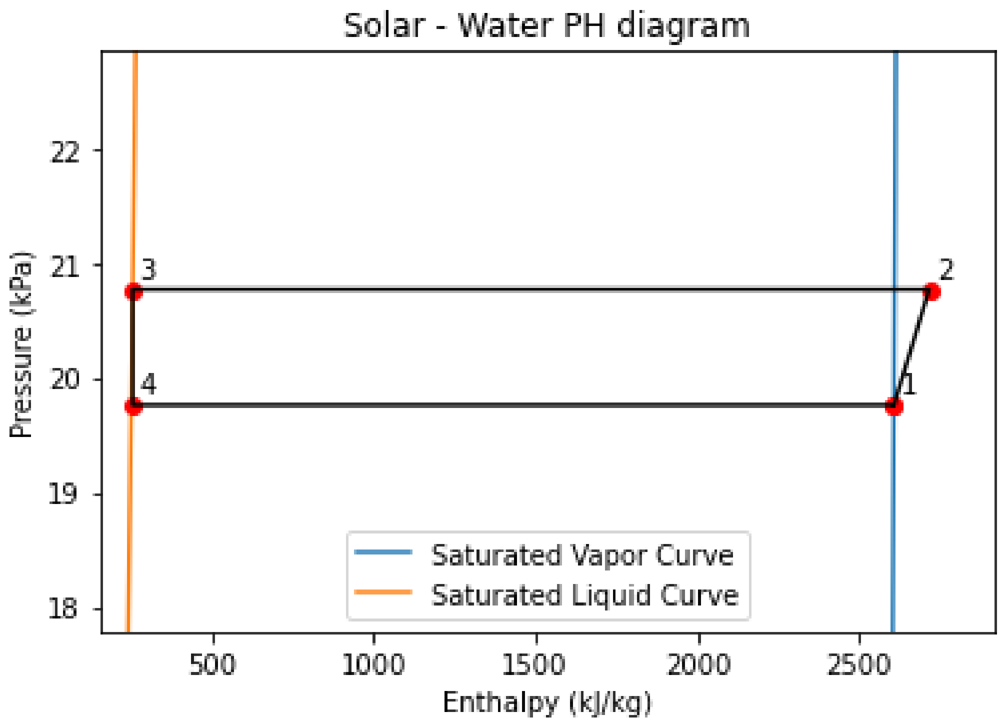

Figure 6: Vapor Compression cycle PH diagram.

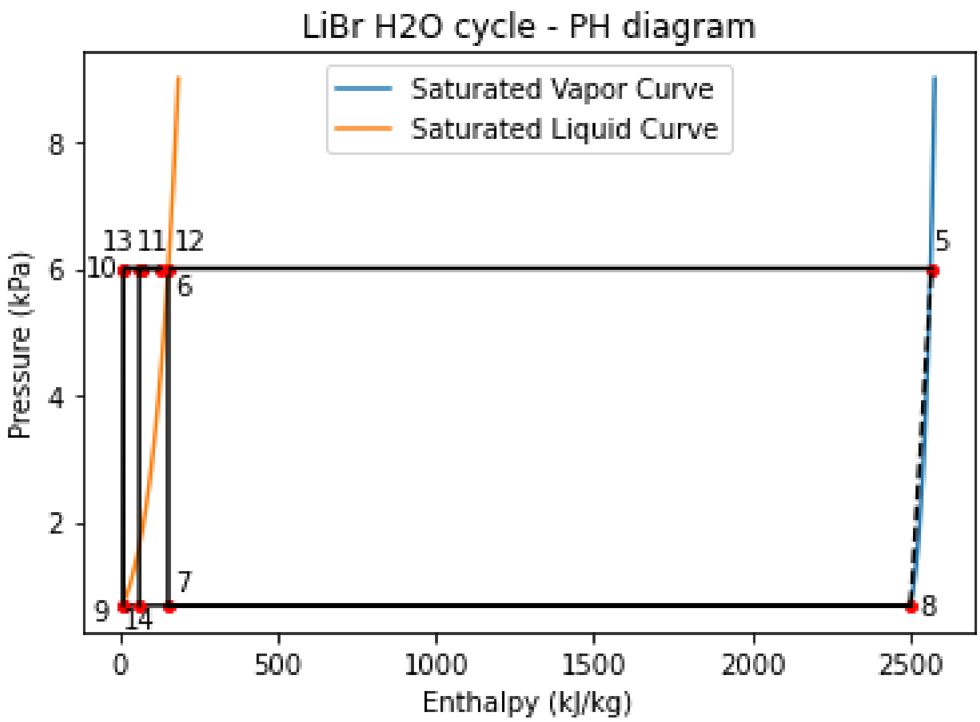

Figure 7: Lithium Bromide absorption cooling PH diagram.

Notably, there is an indirect passage from stream 8 to stream 5 (the black dotted line) on the RHS of Figure 7. This makes up for the 'compressor', which has been replaced by the absorber/desorber of the absorption cycle. This is an indirect path, where the refrigerant actually passes through $8 \rightarrow 9 \rightarrow 10 \rightarrow 11 \rightarrow 5$, where 5 is the superheated vapor. Whilst it may not be explicitly clear, stream 5 is slightly superheated.

The components of the system and overall COP is shown in Table 4 below. The light green cells represent the vapor-compression cycle components, and light blue represents the LiBr-H_2O cycle components.

Table 4: Energy of components for Solar thermal absorption cooling

Component	**Energy – Q (kW)**
Solar Input	8.71
Compressor	0.16
Pump	0.02
Condenser	7.78
Absorber	8.67
Generator	8.86
$COP_{LiBr-H_2O} = 0.85$	

From Table 4, the energy required by the generator is $8.86kW$, to satisfy this, $8.71kW$ is from the solar flat plate collectors, and $0.16kW$ is from the compressor.

The $8.71kW$ solar collector requirement can then be used to size the flat plate collectors in Section 3.3 below.

3.3 Sizing Flat Plate Collectors

Taking the solar average solar irradiance during daylight hours in July (calculated in Section 2.2): $589.89\frac{W}{m^2}$. The total optimal energy received (E_{opt}) is not the same as the Q_{solar} required by this cycle, this is due to losses associated with the collector (Q_{loss}) from convection, conduction, and radiation, hence:

$$Q_{solar} = E_{opt} - Q_{loss}$$

As the inlet and outlet streams of the solar collector are known, along with making a basic collector design, the collect efficiency can be estimated, which can then be applied to find the flat plate collector size. Efficiency can be calculated via:

$$\eta = F_R \tau \alpha - U_t F_R \frac{(T_{in} - T_O)}{I_t}$$

Where: F_R is the heat removal factor, τ is the transmissivity, α is the absorptivity, U_t is a heat loss coefficient, I_t is the solar radiation.

Using a flat plate water collector, with an aluminium absorber with black paint and a double glass cover (Swaminathan N. Handout 2):

$$\eta = 0.9 \times 0.89 - 0.9 \times 4.54 \times \frac{(17.5 - 36)}{589.89}$$

$$\eta = 0.93$$

From this information the size of flat plat collectors via:

$$Flat\ Plate\ Collector\ Size = \frac{Q_{solar}\ Required\ (kW)}{Average\ Irradiance\ \left(\frac{kW}{m^2}\right) \times Collector\ Efficiency}$$

$$Flat\ Plate\ Collector\ Size = \frac{8.71}{0.58989 \times 0.93} = 15.88m^2$$

The floor/roof area for this property was assumed at $70m^2$, hence the $15.88m^2$ is only a fraction of the total roof size.

4. Conclusion and Feasibility

Morocco recently had a unit energy cost of $0.115/kWh (GlobalPetrolPrices. 2023). Cooling a 3-bedroom house (7.56kW cooling load), for 4 hours per day throughout July, costs $107.81. For air conditioning, this price is relatively expensive on a per month basis, furthermore, the costs for the other summer months, e.g. June, August and September are likely to be similar. Providing the solar thermal cooling absorption cycle can be beneficial to residents of Marrakech Morocco by providing them with clean air conditioning, at a low running cost. Finally, 2 key barriers to implementation include; 1. Material and logistical access within Marrakech. 2. The wealth of the locals may not be sufficient to pay for the solar thermal installation.

Further work would include:

- Testing the cycle during the morning hours or evening hours (lower daily irradiance) to understand how this effects the stream concentrations, cooling effect and COP.
- Test performance throughout alternative months.
- Add for solar heating storage for nighttime use – if required.

References

ASHRAE 55. 'Thermal Environmental Conditions for Human Occupancy'. 2010. Accessed at: https://lorisweb.com/LEEDv4/graphics/ASHRAE%20Standards/ASHRAE-D-86150%2055-2010.pdf Accessed on: 14/04/2024.

ASHRAE Morocco. 'Design conditions for CASABLANCA/ANFA, Morocco'. 2005. Accessed at: https://www.bing.com/ck/a?!&&p=445d861eafdfa665JmltdHM9MTcxMTQ5NzYwMCZpZ3VpZD0xMmY4MzQxNi03ZDNlLTZjZjMtM2VhNC0zYjAzN2M3ZTZkYWYmaW5zaWQ9NTIwMw&ptn=3&ver=2&hsh=3&fclid=12f83416-7d3e-6cf3-3ea4-3b037c7e6daf&psq=morocco+dry+bulb+outdoor+temperautre&u=a1aHR0cDovL2Ntcy5hc2hyYWUuYml6L3dlYXRoZXJkYXRhL1NUQVRJT05TLzYwMTU1MF9zLnBkZg&ntb=1 Accessed on: 27/03/2024.

ASHRAE U-values. 'Heat, Air, and Moisture Control in Building Assemblies – Material Properties'. 2021. Accessed at: https://studylib.net/doc/25887787/2021-ashrae-handbook-fundamentals-table-of-u-values Accessed on: 14/04/2024

Assad MEH, Sadeghzadeh M, Ahmadi M H, Al-Shabi M, Albawab M, Moghaddam A A, Hani E B. 'Space cooling using geothermal single-effect water/lithium bromide absorption chiller'. Energy Science & Engineering. Vol 9, Iss 10. pp 1747-1760. 2021. Accessed at: https://doi.org/10.1002/ese3.946 Accessed on: 21/04/2024.

ChemistrySCL. Pyschometric. Accessed at: https://www.chemistryscl.com/higherstudies/chemicalengineering/psychrometric_chart/main.html Accessed on: 27/03/2024.

Climatestotravel. Accessed at: https://www.climatestotravel.com/temperatures/morocco Accessed on: 27/03/2024.

COECS.edu. 'Effect of Infiltration on Latent Load Factor'. Accessed at: https://coecs.ou.edu/Feng.Chyuan.Lai/coolingload/scan/Fig1.PDF Accessed on: 27/03/2024.

DoubleGlazing. 'What is the U value'. Accessed at: https://www.doubleglazing.com/windows/double-glazing-materials/double-glazing-u-value-explained/ Accessed on: 27/03/2024.

EngineeringToolbox. 'Metabolic Heat Gain from Persons.' Accessed at: https://www.engineeringtoolbox.com/metabolic-heat-persons-d_706.html Accessed on: 27/03/2024.

Evapopedia. 'Pyschrometric Chart'. Accessed at: https://evapopedia.com/wet-bulb-temperature/ Accessed on: 14/04/2024.

Faruque M W. 'Calculating thermodynamic properties of lithium bromide solution using Python'. 2020. (Used in the .py script). Accessed at:

https://www.researchgate.net/publication/342702397_Calculating_thermodynamic_properties_of_lithium_bromide_solution_using_Python Accessed on: 21/04/2024.

GlobalPetrolPrices. 'Morocco electricity prices' 2023. Accessed at: https://www.globalpetrolprices.com/Morocco/electricity_prices/ Accessed on: 17/04/2024.

IAPWS R7-97. 'Revised Release on the IAPWS Industrial Formulation 1997 for the Thermodynamic Properties of Water and Steam'. 2012. (Used in the .py script). Accessed at: http://www.iapws.org/relguide/IF97-Rev.pdf Accessed on: 21/04/2024.

Latlong.info. 'Latitiude and longitude of Marrackech'. 2024. Accessed at: https://latlong.info/morocco/marrakech#:~:text=Marrakech%20is%20located%20in%20Morocco%20country%2C%20in%20Africa,Marrakech%20is%20located%20in%20the%20time%20zone%20GMT%2B00. Accessed on: 12/04/2024.

MScCertified. pp 4. Accessed at: https://www.bing.com/ck/a?!&&p=06c681b81472cdccJmltdHM9MTcxMTQ5NzYwMCZpZ3VpZD0xMmY4MzQxNi03ZDNlLTZjZjMtM2VhNC0zYjAzN2M3ZTZkYWYmaW5zaWQ9NTIyOA&ptn=3&ver=2&hsh=3&fclid=12f83416-7d3e-6cf3-3ea4-3b037c7e6daf&psq=stone+wall+U+values&u=a1aHR0cHM6Ly9tY3NjZXJ0aWZpZWQuY29tL3dwLWNvbnRlbnQvdXBsb2Fkcy8yMDIwLzA0L0d1aWRhbmNlLW9uLVUtVmFsdWVzLWZyb20tRG9tZXN0aWMtSGVhdGluZy1EZXNpZ24tR3VpZGUucGRm&ntb=1 Accessed on: 27/03/2024.

MCS. 'Guidance on U-Values from Domestic Heating Design Guide'. 2019. Accessed at: https://mcscertified.com/wp-content/uploads/2020/04/Guidance-on-U-Values-from-Domestic-Heating-Design-Guide.pdf Accessed on: 14/04/2024.

PowerFromTheSun. Accessed at: http://www.powerfromthesun.net/Book/chapter03/chapter03.html#3.2.1%20Solar%20Altitude,%20Zenith,%20and%20Azimuth%20Angles Accessed on: 12/04/2024.

RussellTimberTechnology. Accessed at: https://www.russelltimbertech.co.uk/doors/external-insulated-door-sets Accessed on: 27/03/2024.

SolarSena. 'Solar Hour Angle & How to Calculate it'. 2021. Accessed at: https://solarsena.com/solar-hour-angle-calculator-formula/

Weather Atlas. 'July weather forecast Marrakesh, Morocco'. Accessed at: https://www.weather-atlas.com/en/morocco/marrakesh-weather-july Accessed on: 13/04/2024.